Enhanced Electrokinetic Remediation of Polluted Soils by Anolyte pH Conditioning

López Vizcaíno, R.[a*], Yustres, A.[a], Asensio, L.[a], Saez, C.[b], Cañizares, P.[b], Rodrigo, M.A.[b], Navarro, V.[a]

[a]University of Castilla-La Mancha - Institute of Technology, Campus Universitario s/n, 16071 Cuenca, Spain

[b]Department of Chemical Engineering, Faculty of Chemical Sciences & Technologies, University of Castilla-La Mancha, Campus Universitario s/n, 13071 Ciudad Real, Spain

*** Corresponding author:** ruben.lopezvizcaino@uclm.es; r.lopezvizcaino@gmail.com, University of Castilla-La Mancha - Institute of Technology, Campus Universitario s/n, 16071 Cuenca, Spain

ABSTRACT

In the treatment of a polluted soil, the pH has a strong impact on the development of different physicochemical processes as precipitation/dissolution, adsorption/desorption or ionic exchange. In addition, the pH determines the chemical speciation of the compounds present in the system and, consequently, it conditions the transport processes by which those compounds will move. This question has aroused great interest in the development of pH control technologies coupled to soil remediation processes. In electrokinetic remediation processes, pH has usually been controlled by catholyte pH conditioning with acid solutions, applied to cases of heavy metals pollution. However, this method is not effective with pollutants that can be dissociated in anionic species. In this context, this paper presents a study of the electrokinetic remediation of soils polluted with 2,4-Dichlorophenoxyacetic acid, a common polar pesticide, enhanced with an anolyte pH conditioning strategy. A numerical study is proposed to evaluate the effectiveness of the strategy. Several numerical tests have been carried out for NaOH solutions with different concentrations as pH conditioning fluid. The results show that the anolyte pH conditioning strategy makes it possible to control the pH of the soil and, consequently, the chemical speciation of pollutant species. Thus, it is possible to achieve an important flux of pesticide into the anolyte compartment (electro-migration of anionic species and diffusive transport of acid species). This way, it possible to maximise the pesticide accumulation in this compartment, allowing a much more effective removal of pollutants from the soil than without the anolyte pH conditioning strategy.

KEYWORDS

Electrokinetic soil remediation; Multiphysics simulation; anolyte pH conditioning; pesticide; M4EKR

1. INTRODUCTION

Electrokinetic remediation (EKR) is a technique used in the treatment of polluted soils by which contaminants can be moved to controlled extraction points. This technology is based on the application of an electric field between electrodes placed in the soil, which generates, among other processes, electrokinetic transport mechanisms such as electroosmosis, electromigration and electrophoresis (Acar, 1993; Acar et al., 1995; Virkutyte et al., 2002; Reddy and Cameselle, 2009). One of the main advantages of EKR is that the coupling of these transport processes makes it possible to mobilise fluids, ionic species and/or charged particles in soils with low hydraulic permeability, where Darcy flow is limited. The involvement of several transport mechanisms makes possible to cover a wide range of applications. EKR has been applied in the treatment of soils contaminated with heavy metals (Ottosen et al., 2001; Mascia et al., 2007; Kim et al., 2009), PAH (Pazos et al., 2010; Hahladakis et al., 2014; Bocos et al., 2015) and pesticides (Ribeiro et al., 2005; Ribeiro et al., 2011; Rodrigo et al., 2014; Vieira dos Santos et al., 2016, 2017) obtaining good results.

The action of the electric field also favours certain electrochemical reactions on the surface of the electrodes, especially those leading to water electrolysis. In this process, an important pH gradient is produced due to the generation of protons (H^+) on the anodic surface and hydroxyl ions (OH^-) on the cathodic surface. These ionic species are mobilised through the soil at a rate determined mainly by the electromigration and advective/diffusive processes and the soil's buffering capacity (Acar et al., 1990; Puppala et al., 1997; Reddy et al., 1997; Al-Hamdan and Reddy, 2008b, 2008c; Paz-Garcia et al., 2012a).

The evolution of pH is key in soils treated with EKR, as pH changes induce physicochemical processes beside electrokinetic ones, for example,

precipitation/dissolution of minerals and metals, adsorption/desorption of pollutants and ion exchange between the soil solid skeleton and the pore water. Another aspect to consider is the strong influence of pH on the chemical speciation of the compounds present in the system, both natural substances and pollutant species. The pH determines the ionic form in which a compound is found in the soil. This will indirectly condition the predominant transport process by which this compound will move.

Therefore, the study of pH in EKR processes has aroused a great deal of interest (Zhou et al., 2004b; Gidarakos and Giannis, 2006), since, by controlling this variable, it would be feasible to improve a conventional EKR treatment. The improvements would be related to a controlled chemical speciation and consequently, certain induced transport processes (Yeung and Gu, 2011). Different strategies have been developed focused on pH control (Yeung and Gu, 2011; Gomes et al., 2012) in EKR processes, being electrolyte conditioning one of the most used, especially, catholyte conditioning (Zhou et al., 2004a, 2004b; Yeung and Gu, 2011; Villen-Guzman et al., 2014) in EKR processes for metal removal. In those cases, the conditioning aims to decrease the pH of the catholyte by adding acid species to minimise the precipitation of low mobility salts. However, the anolyte pH conditioning (A-pH-C) has rarely been studied (Saichek and Reddy, 2003; Ryu et al., 2011). This strategy could be of interest when the pollutants can be dissociated in anionic species under basic pH conditions. The study of the application of A-pH-C is the main objective of this work, which presents a numerical analysis of an EKR process in a soil contaminated with 2,4-Dichlorophenoxyacetic acid (2,4-D, a common polar pesticide) using an A-pH-C strategy. NaOH solutions with different concentrations were selected as pH conditioning fluid. The computational module M4EKR, Multiphysics for EKR, (López-Vizcaíno et al., 2017c) has been used to perform this study. M4EKR is a model developed in a multiphysics environment and implemented in COMSOL

Multiphysics (COMSOL, 2015). This tool was developed after extensive research in the field of soil decontamination using EKR processes (Risco et al., 2015; López-Vizcaíno et al., 2016; Risco et al., 2016a, 2016b; López-Vizcaíno et al., 2017a, b). M4EKR allows to characterise and describe the processes that occur during an EKR treatment of a natural soil (López-Vizcaíno et al., 2017c). It has been used to evaluate the transport of water in partially saturated soils subject to an electric field (Yustres et al., 2018) and to analyse the performance of EKR processes enhanced with polarity reversal (López-Vizcaíno et al., 2017d). Thus, it is a tool to study the EKR treatment of soils contaminated with 2,4-D numerically, and evaluate the potential improvements obtained by applying an A-pH-C strategy, which is the main objective of the current research work. This study examines, thanks to the capacities of M4EKR, the temporal evolution of pH and the accumulated pesticide mass, both in the electrolyte compartment and in the soil itself, as well as the spatial distribution of these variables throughout the simulated domain. The mass fluxes of pollutants linked to each transport process are also analysed to improve the overall understanding of each phenomenon and of the EKR process as a whole. As a result, this work obtains valuable information on the behaviour during the EKR of soils contaminated with 2,4-D improved with pH conditioning in anolyte; consequently, it can define guidelines to apply an operating strategy to increase the efficiency of the treatment.

2. CONCEPTUAL MODEL AND NUMERICAL IMPLEMENTATION

The M4EKR module (López-Vizcaíno et al., 2017c) is a reactive transport model for partially saturated porous media. The M4EKR version used in the present study makes several assumptions for conceptual simplification:

- Gas transport was not considered.
- The soil was taken as non-deformable. Soil porosity was considered constant.
- The EKR process took place under isothermal conditions (298.15 K).

- Mineralization processes of the 2,4-D (microbial-mediated degradation and photodegradation) were not considered.
- The 2,4-D adsorption onto the soil was disregarded. The lack of such adsorption has been observed experimentally (Cotillas et al., 2018).

Due to these simplifications, the model does not reproduce the real behaviour of an EKR process. However, this paper does not aim to reproduce perfectly a real behaviour, but to increase the knowledge on how an A-pH-C strategy affects the speciation and transport of pollutants in an EKR process and to evaluate the potential improvements obtained in the efficacy and efficiency of the remediation process. The mathematical formulation used in this M4EKR version is presented in Appendix A. A complete formulation of M4EKR is described in detail in López-Vizcaíno et al. (2017c).

Fig. 1 presents a conceptual model of the system simulated in the tests. This system has a one-dimensional (1D) configuration that allows to obtain clear and easily interpretable results in a shorter simulation time. In this case, a 1D model is a useful tool to make a phenomenological understanding study. This, as previously mentioned, is the main goal of the work.

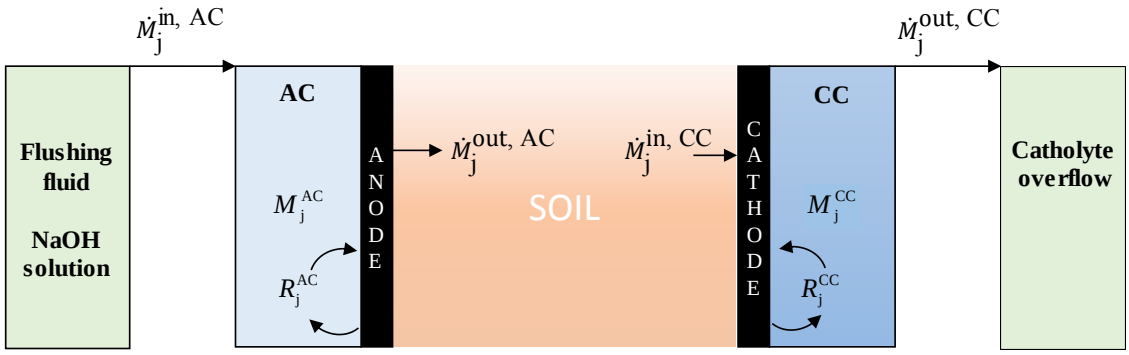

Figure 1. Conceptual model of the one-dimensional domain proposed for simulation.

Two electrolyte compartments have been considered (Anolyte Compartment, AC; Catholyte Compartment, CC) in which the electrodes (anode and cathode, respectively) are located. The function of the electrolyte compartments is double: (i) to collect the pollutants removed from the soil and (ii) to allow adding/extracting the necessary flushing fluid (FF) to maintain a constant level in both electrolyte compartments. The FF is added in the AC, while excess fluid is extracted by overflow in the CC, since the direction of water flow is given by the electroosmotic flux (anode to cathode). A set of different NaOH solutions was used as FF to assess the A-pH-C strategy.

The M4EKR model was implemented in the multiphysics environment solver COMSOL Multiphysics (COMSOL, 2015). COMSOL is a partial differential equation solver that uses the finite element method with Lagrange multipliers. This kind of software is very versatile (Brown et al., 2008; Keyes et al., 2013; Babur et al., 2015), allowing the modeller to define the system of differential and algebraic equations to solve. An important novelty of this work is that the system of equations used to calculated the chemical speciation problem is integrally solved by the M4EKR module in COMSOL (monolithic approach), as opposed to common operator-splitting procedures that couple other reactive transport codes (Carrayrou et al., 2004; Jacques et al., 2006; Paz-García et al., 2012b). In addition, the system of ordinary differential equations that define the mass balance in electrolyte wells, Eq. (A.11), is solved together with the partial differential equations that determine the balance of water, species and electric charge (Eqs. (A.1), (A.9) and (A.10), respectively). This complex calculation is possible thanks to the great flexibility that COMSOL (COMSOL, 2015) provides to the M4EKR module.

3. SIMULATION OF THE EKR PROCESS

3.1. Modelled configuration

3.1.1. Polluted Soil

The studied soil is a material from a quarry in Toledo (Spain), which is classified as a low-plasticity clay (CL) according to the Unified Soil Classification System. It is composed of smectite (28%), kaolinite (26%), illite (20%), feldspar (15%), quartz (7%) and calcite (4%). The particle size distribution of the soil shows an important silt fraction (68.2%), a minor fraction of sand (26.9%) and a low fraction of clay (4.9%). A bulk density of 1.89 g/mL and a gravimetric water content of 32.8% were assumed to represent compaction conditions representative of the natural state of this soil (López-Vizcaíno et al., 2016). The soil parameters used in the simulations are presented as Supplementary Material, Table SM-1. The procedure used to determine the water retention curve parameters is described in Yustres et al. (2018).

3.1.2. Pore water

A synthetic pore water was simulated using a geochemical model of 5 components and 9 species. Table SM-2 presents the equilibrium reactions involved, their respective equilibrium constants (Giffaut et al., 2014) and physicochemical properties, as well as hard-core diameters and diffusion coefficients, obtained both from literature and estimated with Pikal's expression (Pikal, 1971). The WATEQ Debye-Hückel model (Parkhurst and Appelo, 1999) was used to determine the activity coefficients.

3.1.3. Modelled Experimental setup

An EKR reactor was simulated, composed of an electrochemical cell formed by two electrolyte compartments of 135 mL (LWH: 15×3×3 cm) and a central compartment of

675 mL (LWH: 15×15×3 cm) to contain the contaminated soil. This modelled experimental setup is the same as that used in previous works, in which a more detailed description can be found (López-Vizcaíno et al., 2017c, 2017d).

3.1.4. Initial conditions

The initial electrolyte is an aqueous NaCl solution (9.53×10^{-4} m) with a neutral pH (7). The initial soil pore water has the same concentration of NaCl and an additional amount of 2,4-D corresponding to the initial pollution target in soil (20 mg $\mathrm{kg}^{-1}_{\mathrm{dry\ soil}}$). The total ionic strength, IS, of the initial soil pore water is 9.53×10^{-4} m. The FF used are solutions of NaOH of different concentrations (0.01 to 0.025 m). The initial liquid pressure, $P_{L,}$ was fixed at 100 kPa and the initial electric potential was 1 V. Table 1 presents the values of the initial conditions selected in the cases evaluated in this work.

Table 1. Initial conditions.

	Total component concentration / m			**pH**	**IS / m**
	H+	**Na+**	**2,4-D$_{anion}$**		
Soil pore water	1.65×10^{-8}	9.53×10^{-4}	3.19×10^{-4}	7.00	9.53×10^{-4}
Electrolyte	-3.06×10^{-11}	9.53×10^{-4}	0.00	7.00	9.53×10^{-4}
FF 0.01 m NaOH	-1.00×10^{-2}	1.09×10^{-2}	0.00	11.95	1.09×10^{-2}
FF 0.0125 m NaOH	-1.25×10^{-2}	1.35×10^{-2}	0.00	12.05	1.32×10^{-2}
FF 0.015 m NaOH	-1.50×10^{-2}	1.59×10^{-2}	0.00	12.12	1.59×10^{-2}
FF 0.0175 m NaOH	-1.75×10^{-2}	1.85×10^{-2}	0.00	12.18	1.84×10^{-2}
FF 0.02 m NaOH	-2.00×10^{-2}	2.09×10^{-2}	0.00	12.24	2.09×10^{-2}
FF 0.025 m NaOH	-2.50×10^{-2}	2.59×10^{-2}	0.00	12.33	2.58×10^{-2}

3.1.5. Boundary conditions

For the electric charge balance equation, an electric gradient of 1 V cm^{-1} was imposed in all cases as boundary condition. For the water mass balance, P_L was maintained constant and equal to the atmospheric pressure (100 kPa) in the boundaries. Finally, for the balance of the chemical components, the concentration of the components in the electrolyte

compartments was imposed in the boundaries. These concentrations are obtained by the coupled calculation of the *J-2* ordinary differential equations used to solve the mass balance of the chemical components in the electrolyte wells.

3.2. Simulation of EKR tests

Seven EKR tests have been simulated to analyse the behaviour of the system under an A-pH-C strategy. The difference between the simulated tests was the NaOH concentration in the FF (see Table SM-3). This way, the first test was simulated, as a reference, using a FF solution without NaOH and the salts concentration of the initial electrolyte (see Table 1). The following six tests were performed using FF solutions with an increasing NaOH concentration (0.01, 0.0125, 0.015, 0.0175, 0.02 and 0.025 m). This work aims to evaluate the performance of an EKR process conditioning the pH of the anolyte, focusing the study on the analysis of the transition period. This stage is the most important of the test because it will characterise the different responses produced by the A-pH-C strategy. For this reason, the duration of the test will be different in each simulation. It will correspond to the time necessary to achieve a "pseudo stationary" state in the evaluated process, that is, when the pH spatial distribution remains constant in the domain. Fig. 2 shows the temporal evolution of pH in the two electrolyte compartments.

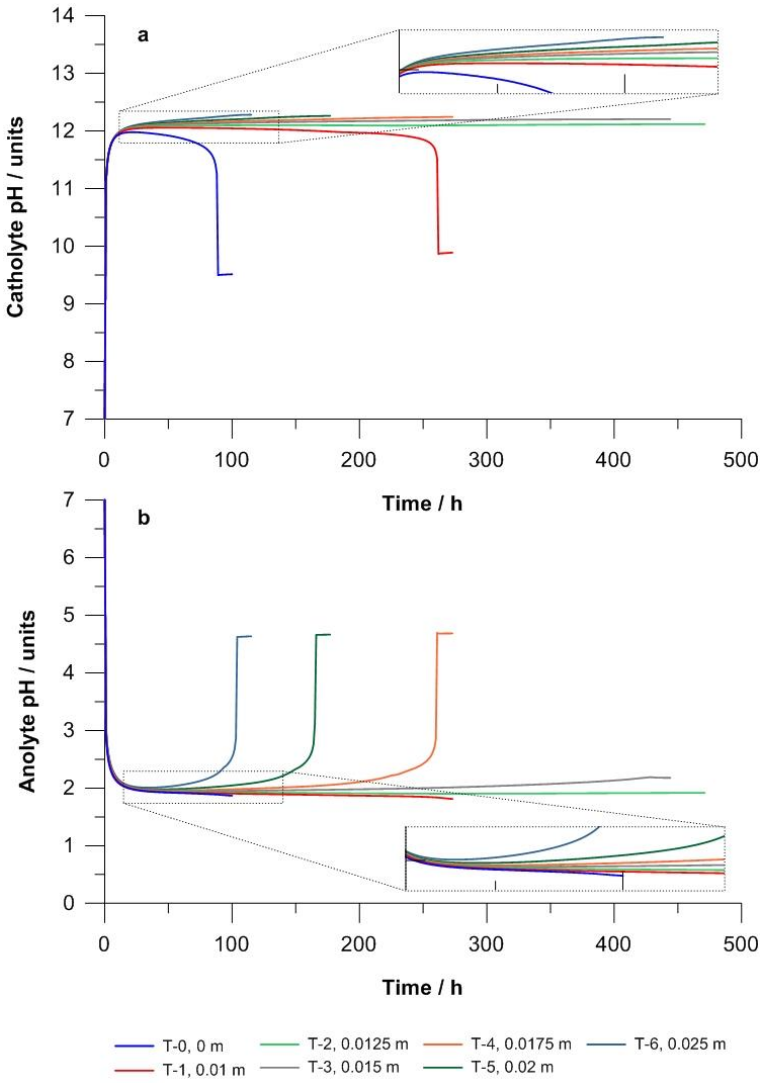

222

223 **Figure 2.** Dynamic response of pH in (a) catholyte and (b) anolyte compartments.

224

225 The pH temporal evolution observed in the simulations is characteristic of EKR
226 processes. Basification occurs in the CC, because hydroxyl ions are electrogenerated in
227 the water reduction reaction derived from electrolysis. The pH increases from 7 up to
228 nearly 12 in a very short time. In the same way, the opposite process (electrogeneration
229 of protons during water oxidation) occurs in the AC, where a pH drops strongly, to values
230 close to 2.

In addition, different trends over time can be identified in five of the tests. Tests T-0 and T-1 later show a rapid change in the pH of the CC, decreasing from approximately 12 to 9.5 and 9.8 at 89 and 262 h, respectively. After these times, the catholyte pH is stabilised. These temporal points coincide with the arrival of an acid pH front to the CC. The behaviour shown by T-0 was observed in a previous work (López-Vizcaíno et al., 2017d) where A-pH-C was not applied. Although it takes more time for the acid pH front to reach the CC, analogous performance is obtained in T-1 (A-pH-C with 0.01 m NaOH). This indicates that the NaOH solution used as FF partially neutralises the protons produced in the AC but the NaOH concentration is insufficient to increase the pH of the soil.

On the other hand, tests T-4, T-5 and T-6 present an anolyte pH evolution contrasting with that of T-0 and T-1. After the first stage, a sudden rise of the pH to nearly 4.5 is observed. Then, pH stabilises at 261 h, 166 h and 104 h, respectively. This behaviour can be explained in the same terms used before. In these cases, the NaOH concentration of the FF is higher than in the previous tests, and it can completely neutralise the acid front generated in the AC. In this concentration range (0.0175-0.025 m), the amount of NaOH added in the AC affects the time necessary for the basic pH front to be transported from the CC to the AC.

Tests T-2 and T-3 present evolutions different to the previous ones. After the first stage, the pH in the AC and the CC remains in values close to 2 and 12, respectively, all throughout the test.

To illustrate these trends of behaviour, the pH spatial distribution in the soil is plotted in Figures 3A and 3B at two times, 42 and 84 h. Moreover, the spatial distribution of the concentration of the two pesticide species, anionic species (2,4-D_{anion}) and acid species (2,4-D_{acid}), at the mentioned times, is presented in Figs. 3c, 3d and Figs. 3e, 3f, respectively.

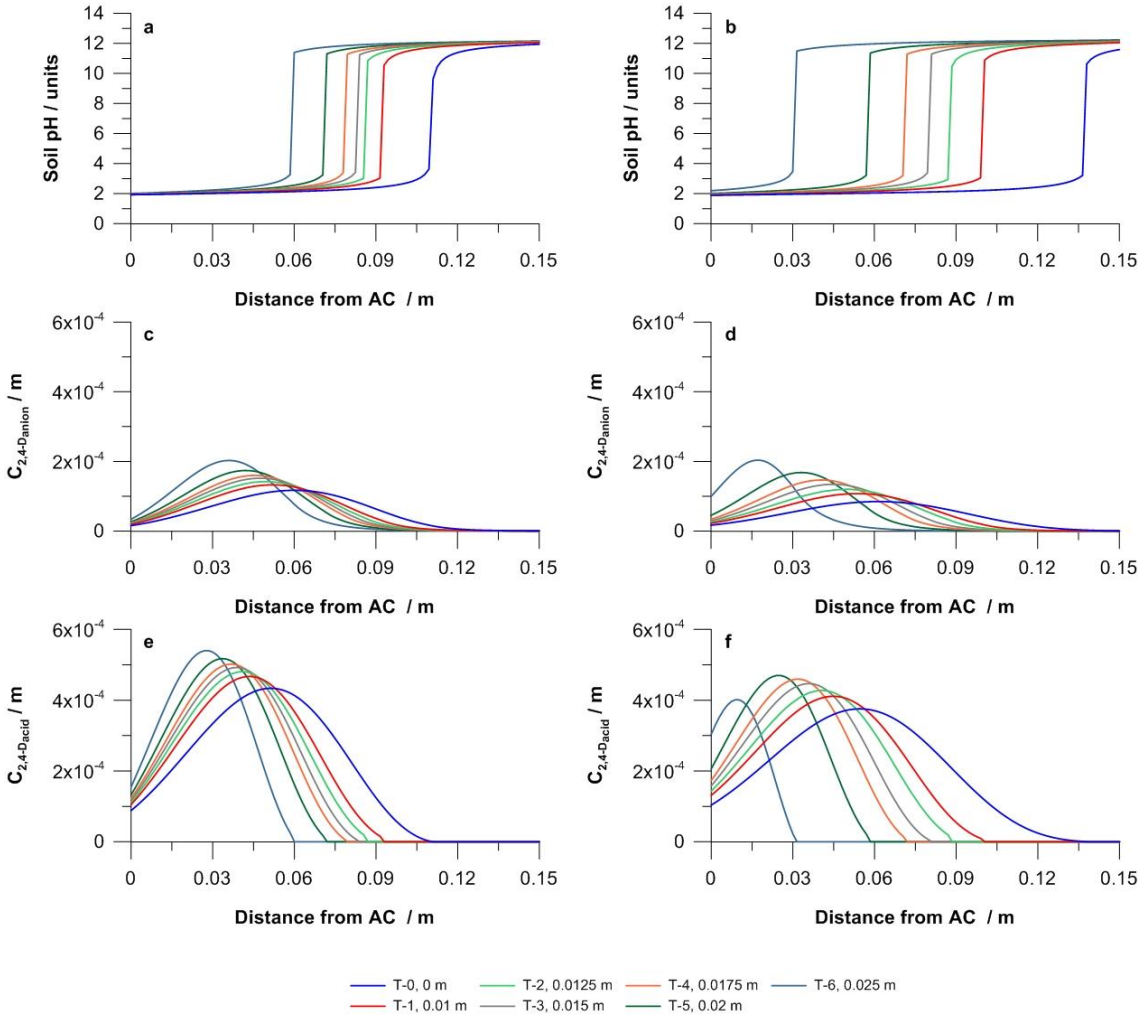

Figure 3. Spatial distribution in the EKR study with an A-pH-C strategy of the (a, b) pH, (c, d) total concentration of the 2,4-D_{anion} species, and (e, f) total concentration of the 2,4-D_{acid} species. Evaluated times: (a, c, e) 42 h and (b, d, f) 84 h.

In all the studied cases, the pH spatial distribution shows the characteristic evolution of an electrochemical cell, with an important pH gradient between anode and cathode. Taking the first evaluated time, 42 h (Fig. 3a), as a reference, an increase of the NaOH concentration in FF slows down the displacement of the acid front towards the CC due to the neutralization of protons. The pH front reaches a distance of 0.11 m in test T-0, and only of 0.06 m in test T-6. This is consistent with the previous explanation of the dynamic response of the pH electrolytes. Moreover, analysing the second time, 84 h (Fig. 3b), the

phenomenon is more evident, since the pH front is mobilised towards the CC in T-0 and towards the AC in T-6. These observations agree with the trend of pH changes shown in Fig. 2.

The pH strongly influences the chemical speciation of the substances presents in the soil (Al-Hamdan and Reddy, 2008a, 2008b). There is a direct relation between pH and chemical speciation. Acid species are only present between the anolyte and the pH front. This zone can be termed acid region. The extent of this region shrinks when the NaOH concentration increases in the FF (Figs. 3a and 3b). This shrinkage has two important effects: (i) the predominant pollutant species, 2,4-D_{acid}, is concentrated very effectively near the AC (Fig. 3d), and (ii) the transformation of 2,4-D_{acid} to 2,4-D_{anion} is improved (Fig. 3f). Taking into account these two considerations, the A-pH-C strategy favours the presence of a relevant amount of 2,4-D anion species close to the AC, which is susceptible of being mobilised towards the AC by the more effective electromigration process.

To improve our knowledge of how 2,4-D is mobilised, its mass fluxes have been analysed. The fluxes associated with each transport process are independently evaluated at the soil/AC interface (Fig. 4). A similar study in the soil/CC interface is not presented because the pesticide concentration is negligible in this zone (Figs. 3a and 3b); therefore, the mass fluxes in the soil/CC interface are negligible compared to those obtained in the soil/AC interface.

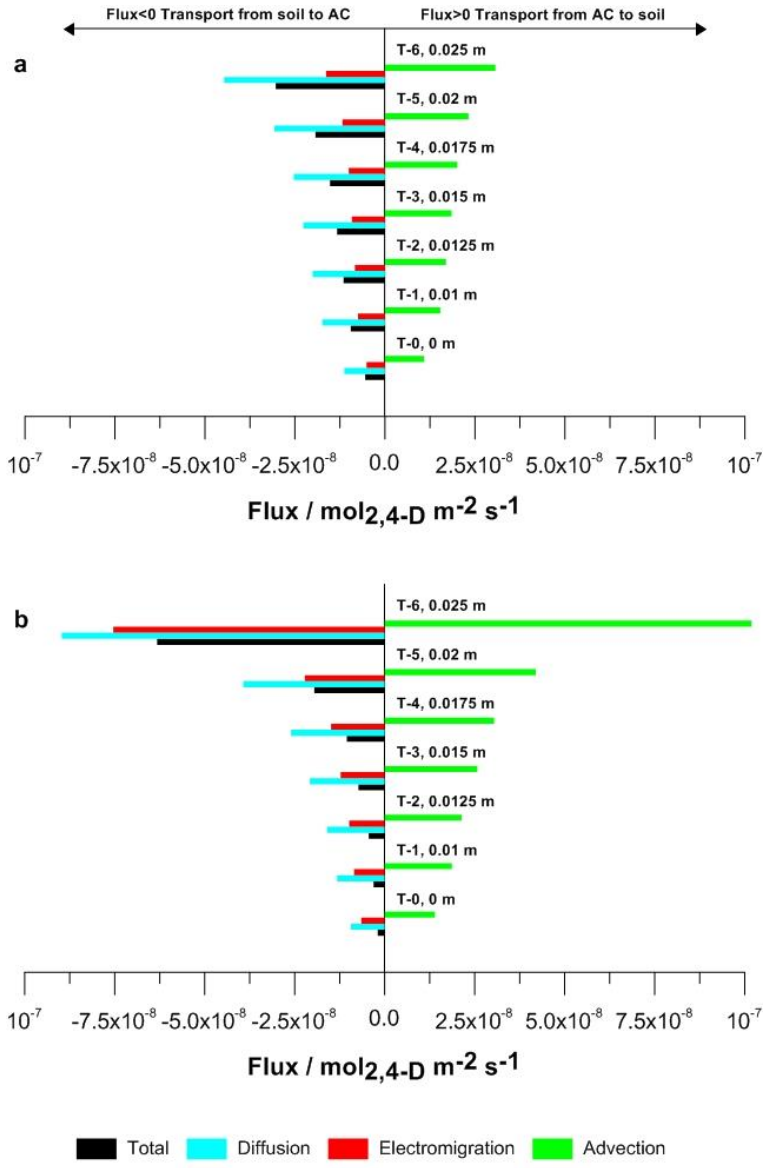

287

288 **Figure 4**. Total mass fluxes for the 2,4-D component at the AC/soil interface. Evaluated times:
289 (a) 42 h and (b) 84 h.

290 The total mass fluxes obtained in the tests with lower NaOH concentrations (T-0 to T-3)
291 are more similar to each other than to the rest at the two times analysed. However, tests
292 T-4 to T-6 show a notable flux increase at 84 h, especially T-6, where the total flux
293 increases one order of magnitude. This trend is explained after the spatial distribution of
294 the total concentration of the anionic and acid species of the pesticide (Fig. 3), both of
295 which show an increase close to the AC/soil interface. This favours the diffusive flux of
296 anionic and acid species towards the AC (where the pesticide concentration is lower), the

297 electromigration flux of the anionic species towards the AC and the advective (hydraulic
298 and electroosmotic) flux of anionic and acid species towards the CC.

299 Analysing the fluxes associated with each transport process, the A-pH-C strategy
300 improves the electromigration process because of the dissociation of the acid species into
301 the anionic species. In addition, the shrinkage of the acid region produces an accumulation
302 of the acid species near the AC, increasing the diffusive fluxes. The combination of these
303 phenomena produces a net mass flux towards the AC, which increases with the NaOH
304 concentration in the FF.

305 The dynamic response of the concentration of 2,4-D in the AC has also been analysed
306 (Fig. 5) to check the effects of the pesticide transport along the total test time. In general
307 terms, an increase in the total mass flux towards the AC produces an important increase
308 of pesticide concentration in this electrolyte compartment. This response is more
309 noticeable in the A-pH-C tests with a NaOH concentration greater than 0.015 m.

310 After an individual analysis, tests T-0, T-1 and T-2 show a quick increase in the total 2,4-
311 D concentration during the first 50 h of the tests, which is then stabilised. The
312 predominant accumulated species is 2,4-D_{acid}, mainly from diffusive transport (Fig. 4).
313 When the pesticide concentrations in the electrolyte compartments and in the soil become
314 equal, the initial concentration gradient has been reduced, and consequently the diffusive
315 flux is lower. This produces the stated stabilization of the 2,4-D concentration in time.
316 The contribution of the pesticide anionic species is very low, consistently with the lower
317 electromigration flux in these tests (Fig. 4).

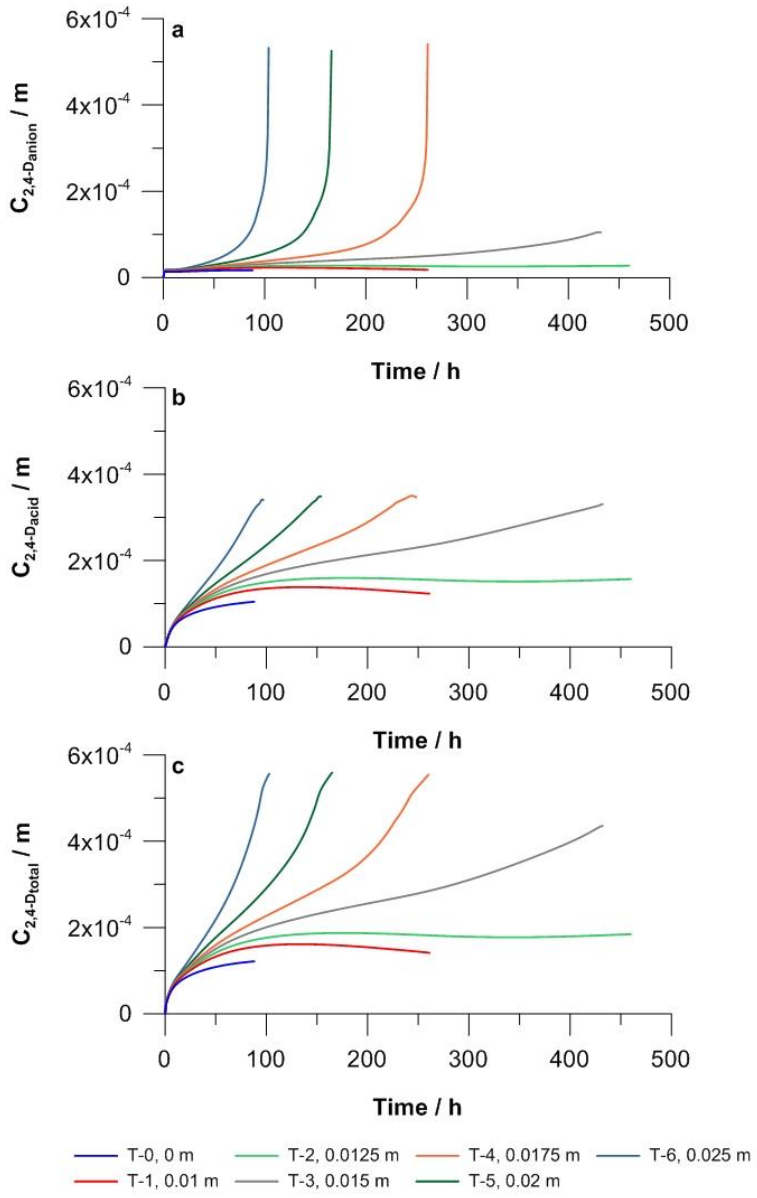

318

319 **Figure 5.** Dynamic response of the concentration of 2,4-D (a) anionic species, (b) acid species
320 and (c) total component in the AC.

321 On the other hand, tests T-4, T-5 and T-6 present an important increase along time in the
322 total 2,4-D concentration in the AC (Fig. 3). The reason is twofold: (i) the accumulation
323 of the 2,4-D_{acid} species close to the AC induces a large concentration gradient, and
324 therefore the diffusive transport occurs along the entire test (Fig. 5b); and (ii) the A-pH-
325 C strategy favours in these cases the chemical speciation towards the 2,4-D_{anion},

consequently improving the contribution of electromigration to the total transport of pesticide (Fig. 5a).

The last point evaluated is the quantification of the improvements derived from the A-pH-C strategy applied in the EKR of polluted soils with 2,4-D. To do this, the efficiency of the enhanced EKR process has been analysed evaluating the mass of pesticide remaining in the AC, the CC and the soil after the treatment (Fig. 6).

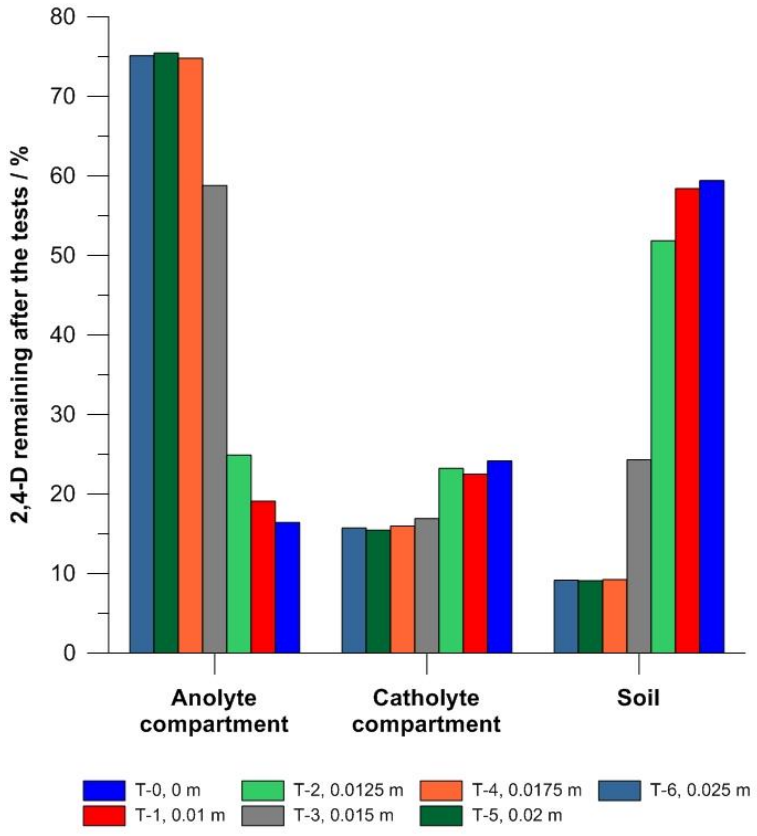

Figure 6. Distribution of 2,4-D after the EKR tests enhanced with A-pH-C.

The reference test (T-0) is the least efficient. A 59% of the initial pesticide mass remains in the soil and only a 24% and a 17 % are accumulated in the CC and the AC, respectively. In tests T-1 and T-2, the mass of 2,4-D in soil drops up to a 50%, that in the CC is approximately the same, and that in the AC increases up to a 25%. The rest of tests (T-3

to T-6) obtain only a 10% of the initial pesticide mass remaining in the soil. The pollutant is accumulated mainly in the AC, achieving a 75% of the initial mass for a NaOH concentration of 0.0175 m in the FF. For higher NaOH concentrations, the results regarding pesticide removal are the same, but the time necessary to achieve them is reduced significantly (from 261 to 104 h, see Table SM-3). This fact confirms that the A-pH-C strategy improves notably EKR processes applied to the treatment of a soil polluted with 2,4-D.

4. CONCLUSIONS

This work presents a numerical study to analyse the effects of an Anolyte pH Conditioning (A-pH-C) strategy in the electrokinetic remediation of a soil polluted with 2,4-D pesticide. Seven numerical tests have been studied, using NaOH aqueous solutions with different concentrations as flushing fluid (added to the anolyte compartment). The results show that the A-pH-C strategy allows to control the soil pH indirectly, slowing the advance of the acid front towards the catholyte compartment because of the neutralization of protons derived from anodic water oxidation. Consequently, the chemical speciation is affected by A-pH-C. The 2,4-D_{acid} species is accumulated in the acid region of the soil (close to the anolyte compartment), and the dissociation of the acid species towards the 2,4-D_{anion} species is favoured due to the important pH increase produced by adding NaOH. These effects result in the development of a large net mass flux towards the anolyte compartment (mainly of the anionic species by electromigration and of the acid species by diffusive flux), allowing a much more effective pesticide removal from the soil than in the reference test (without the A-pH-C strategy). Finally, in the cases studied, a minimum concentration of NaOH is needed to obtain this improvement in the EKR process. Higher NaOH concentrations than the minimum do not improve the pesticide removal, but can reduce the time needed to achieve the same results.

ACKNOWLEDGEMENTS

Financial support from the Spanish Ministry of Economy, Industry and Competitiveness and the European Union through project [CTM2016-76197-R (AEI/FEDER, UE)] and from Junta de Comunidades de Castilla - La Mancha through the Postdoctoral Grant [(SBPLY/16/180501/000402)] awarded to Dr. López-Vizcaíno are gratefully acknowledged.

APPENDIX A

A.1. Water mass balance

Eq. (A.1) defines the water mass balance in a soil domain:

$$\frac{\partial m_w}{\partial t} + \nabla \cdot \mathbf{l}_w = 0 \quad \text{(A.1)}$$

where m_w is the mass of water per unit total volume (kg m^{-3}), $\nabla\cdot$ is the divergence operator, and $\mathbf{l}_w$ is the mass flux of water (kg m^{-2} s^{-1}). The term m_w is defined as:

$$m_w = \phi \cdot Sr \cdot \rho_w + \phi \cdot (1 - Sr) \cdot \rho_v \quad \text{(A.2)}$$

where ϕ is the soil porosity, ρ_w is the water density (kg m^{-3}), the degree of saturation of the soil, *Sr*, is estimated using the van Genuchten model (van Genuchten, 1980), and ρ_v is the density of water vapour (kg m^{-3}), which is calculated with the psychrometric equation (Edlefsen and Anderson, 1943):

$$\rho_v = \rho_v^0 \cdot exp\left(\frac{M_w \cdot s}{\rho_w \cdot R \cdot T}\right) \quad \text{(A.3)}$$

where M_w is the molar mass of water, T is the temperature and *s* is the matric suction (osmotic suction is not considered), which is given by the difference between the gas phase pressure and the liquid phase pressure.

385 The flux term $\mathbf{l}_w$, Eq. (A.4) is calculated as the sum of the hydraulic flux ($\mathbf{l}_w^h$), which is

386 calculated with Darcy's law, and the electroosmotic flux ($\mathbf{l}_w^{eo}$), which is computed with

387 the semi-empirical model of Helmholtz-Smoluchowski (Mitchell and Soga, 2005).

388 $$\mathbf{l}_w = \mathbf{l}_w^h + \mathbf{l}_w^{eo} = \rho_w \cdot \left(\mathbf{q}_w^h + \mathbf{q}_w^{eo}\right) = \rho_w \cdot \mathbf{q}_w \quad \text{(A.4)}$$

389 where $\mathbf{q}_w^h$ and $\mathbf{q}_w^{eo}$ are the hydraulic and electroosmotic volumetric fluxes (see Eqs. (A.5)

390 and (A.7) respectively).

391 $$\mathbf{q}_w^h = -K_e^h \cdot (\nabla P_L + g \cdot \rho_w \cdot \nabla z) \quad \text{(A.5)}$$

392 $$K_e^h = K_{sat}^h \cdot k_{rel} = K_{sat}^h \cdot Sr^3 \quad \text{(A.6)}$$

393 $$\mathbf{q}_w^{eo} = -K_e^{eo} \cdot \nabla E \quad \text{(A.7)}$$

394 $$K_e^{eo} = K_{sat}^{eo} \cdot k_{rel} = K_{sat}^{eo} \cdot Sr^3 \quad \text{(A.8)}$$

395 where K_e^h is the effective hydraulic permeability of the soil, which is calculated by

396 multiplying the saturated permeability (K_{sat}^h) by a relative permeability function.

397 Additionally, ∇ is the gradient differential operator, g is gravity, z is the vertical

398 coordinate, E is the electric potential, K_e^{eo} is the effective electro-osmotic permeability

399 of the soil, which is calculated using the same formulation employed in the calculation of

400 K_e^h, and K_{sat}^{eo} is the saturated electro-osmotic permeability. A Brooks and Corey-type

401 power function (Brooks and Corey, 1964) with an exponent of 3 was chosen for both

402 relative permeability functions.

403

404

A.2. Reactive transport

The M4EKR module considers a geochemical system composed of *J* components able to produce a total of *N* chemical species for the chemical reactions contemplated (Bethke, 2007). This way, to know the total chemical composition of the system, it is necessary to calculate the total amount of each *j* component (*j*=1...*J*) using a general mass balance equation:

$$\frac{\partial m_j}{\partial t} + \nabla \cdot \mathbf{l}_j = R_j \qquad \text{(A.9)}$$

where m_j is the total mass of component *j* per unit total volume (mol m^{-3}), $\mathbf{l}_j$ is its total molar flux (mol m^{-2} s^{-1}), and R_j is its rate of production or consumption (mol m^{-3} s^{-1}). The flux $\mathbf{l}_j$ is calculated as the sum of the contributions of four transport processes: advective transport generated by (i) hydraulic, (ii) electroosmotic and (iii) electromigration fluxes, and (iv) Fickian diffusive-dispersive transport. Only *J-2* partial differential equations are needed to be solved, because the total mass of one of the components is computed after electroneutrality and Eq. (1) is used for H_2O.

A classical stoichiometric approach based on a system of mass-balance and mass-action equations was used to solve the chemical speciation problem (Leal et al., 2014). The general formulation of this method has been extensively defined in others works (Lichtner, 1985; Parkhurst and Appelo, 1999; Bethke, 2007; Steefel et al., 2015). The specific equations used in M4EKR can be found in literature (López-Vizcaíno et al., 2017c; López-Vizcaíno et al., 2017d).

A.3. Electric charge balance

The electroneutrality condition is met throughout the domain. Moreover, the system has not charge accumulation capacity. With these assumptions, the balance equation of the total electric charge is defined by Eq. (A.10):

$$\nabla \cdot \mathbf{i} = 0 \qquad \text{(A.10)}$$

where **i** is the total current density (A m^{-2}), which is calculated by applying Ohm's law (Jacobs and Probstein, 1996; López-Vizcaíno et al., 2017c). The apparent electrical conductivity of the soil and electrical conductivity of pore water are estimated with the formulation of Rhoades (Rhoades et al., 1989) and Appelo and Postma (Appelo and Postma, 2004), respectively. These formulations are described in López-Vizcaíno et al. (2017c).

A.4. Mass balance in electrolyte wells

Assuming that the electrolyte compartments behave like ideal continuous stirring tank reactors, J-2 balance equations, Eq. (A.11), must be solved in each compartment to calculate the mass evolution of the J components:

$$\frac{dM_j^*}{dt} = \dot{M}_j^{in,*} - \dot{M}_j^{out,*} + R_j^* \qquad \text{(A.11)}$$

where superscript * is equal to AC or CC depending on the electrolyte compartment, R_j^* is the source/sink term (mol s^{-1}) subject to the electrochemical reactions considered (redox reactions linked to water electrolysis), M_j^* is the total mass of component *j* (mol) and denotes the mass of component *j* per unit time (mol s^{-1}) being added (superscript *in*) or extracted (superscript *out*) to the electrolyte compartment studied. The formulation used to calculate these variables is described in a previous work (López-Vizcaíno et al., 2017c).

REFERENCES

Acar, Y.B., 1993. Principles of electrokinetic remediation. Envir. Sci. Tech. 27, 2638-2647.

Acar, Y.B., Gale, R.J., Alshawabkeh, A.N., Marks, R.E., Puppala, S., Bricka, M., Parker, R., 1995. Electrokinetic remediation: Basics and technology status. J. Hazard. Mater. 40, 117-137.

Acar, Y.B., Gale, R.J., Putnam, G.A., Hamed, J., Wong, R.L., 1990. Electrochemical processing of soils: Theory of ph gradient development by diffusion, migration, and linear convection. J. Environ. Sci. Health Part A Environ. Sci. Eng. Toxic Hazard. Subst. Control 25, 687-714.

Al-Hamdan, A.Z., Reddy, K.R., 2008a. Electrokinetic remediation modeling incorporating geochemical effects. J. Geotech. Geoenviron. Eng. 134, 91-105.

Al-Hamdan, A.Z., Reddy, K.R., 2008b. Geochemical assessment of metal transport in glacial till during electrokinetic remediation. Environ. Monit. Assess. 139, 137-149.

Al-Hamdan, A.Z., Reddy, K.R., 2008c. Transient behavior of heavy metals in soils during electrokinetic remediation. Chemosphere 71, 860-871.

Appelo, C.A.J., Postma, D., 2004. Geochemistry, Groundwater and Pollution, Second Edition. CRC Press.

Babur, Ö., Smilauer, V., Verhoeff, T., Van Den Brand, M., 2015. A survey of open source multiphysics frameworks in engineering. Procedia Comput. Sci., 1088-1097.

Bethke, C.M., 2007. Geochemical and Biogeochemical Reaction Modeling. Cambridge University Press.

Bocos, E., Fernández-Costas, C., Pazos, M., Sanromán, M.Á., 2015. Removal of PAHs and pesticides from polluted soils by enhanced electrokinetic-Fenton treatment. Chemosphere 125, 168-174.

Brooks, R.H., Corey, A.T., 1964. Hydraulic Properties of Porous Media. Colorado State University.

Brown, D.L., Bell, J., Estep, D., Gropp, W., Hendrickson, B., Keller-McNulty, S., Keyes, D., Oden, J.T., Petzold, L., Wright, M., 2008. Applied Mathematics at the U.S. Department of Energy: Past, Present and a View to the Future. IAEA-INIS Repository.

Carrayrou, J., Mosé, R., Behra, P., 2004. Operator-splitting procedures for reactive transport and comparison of mass balance errors. J. Contam. Hydrol. 68, 239-268.

COMSOL, A., 2015. COMSOL Multiphysics Reference Manual Version: COMSOL 5.1.

Cotillas, S., Sáez, C., Cañizares, P., Cretescu, I., Rodrigo, M.A., 2018. Removal of 2,4-D herbicide in soils using a combined process based on washing and adsorption electrochemically assisted. Sep. Purif. Technol. 194, 19-25.

Edlefsen, N., Anderson, A., 1943. Thermodynamics of soil moisture. Hilgardia 15 (2), 31-298.

Gidarakos, E., Giannis, A., 2006. Chelate agents enhanced electrokinetic remediation for removal cadmium and zinc by conditioning catholyte pH. Water Air Soil Poll. 172, 295-312.

Giffaut, E., Grivé, M., Blanc, P., Vieillard, P., Colàs, E., Gailhanou, H., Gaboreau, S., Marty, N., Madé, B., Duro, L., 2014. Andra thermodynamic database for performance assessment: ThermoChimie. Appl. Geochem. 49, 225-236.

Gomes, H.I., Dias-Ferreira, C., Ribeiro, A.B., 2012. Electrokinetic remediation of organochlorines in soil: Enhancement techniques and integration with other remediation technologies. Chemosphere 87, 1077-1090.

Hahladakis, J.N., Lekkas, N., Smponias, A., Gidarakos, E., 2014. Sequential application of chelating agents and innovative surfactants for the enhanced electroremediation of real sediments from toxic metals and PAHs. Chemosphere 105, 44-52.

Jacobs, R.A., Probstein, R.F., 1996. Two-Dimensional Modeling of Electroremediation. AIChE Journal 42, 1685-1696.

Jacques, D., Šimůnek, J., Mallants, D., van Genuchten, M.T., 2006. Operator-splitting errors in coupled reactive transport codes for transient variably saturated flow and contaminant transport in layered soil profiles. J. Contam. Hydrol. 88, 197-218.

Keyes, D.E., McInnes, L.C., Woodward, C., Gropp, W., Myra, E., Pernice, M., Bell, J., Brown, J., Clo, A., Connors, J., Constantinescu, E., Estep, D., Evans, K., Farhat, C., Hakim, A., Hammond, G., Hansen, G., Hill, J., Isaac, T., Jiao, X., Jordan, K., Kaushik, D., Kaxiras, E., Koniges, A., Lee, K., Lott, A., Lu, Q., Magerlein, J., Maxwell, R., McCourt, M., Mehl, M., Pawlowski, R., Randles, A.P., Reynolds, D., Rivière, B., Rüde, U., Scheibe, T., Shadid, J., Sheehan, B., Shephard, M., Siegel, A., Smith, B., Tang, X., Wilson, C., Wohlmuth, B., 2013. Multiphysics simulations: Challenges and opportunities. Int. J. High Perform. Comput. Appl. 27, 4-83.

Kim, D.H., Ryu, B.G., Park, S.W., Seo, C.I., Baek, K., 2009. Electrokinetic remediation of Zn and Ni-contaminated soil. J. Hazard. Mater. 165, 501-505.

Leal, A.M.M., Blunt, M.J., LaForce, T.C., 2014. Efficient chemical equilibrium calculations for geochemical speciation and reactive transport modelling. Geochim. Cosmochim. Acta. 131, 301-322.

Lichtner, P.C., 1985. Continuum model for simultaneous chemical reactions and mass transport in hydrothermal systems. Geochim. Cosmochim. Acta. 49, 779-800.

López-Vizcaíno, R., Navarro, V., León, M.J., Risco, C., Rodrigo, M.A., Sáez, C., Cañizares, P., 2016. Scale-up on electrokinetic remediation: Engineering and technological parameters. J. Hazard. Mater. 315, 135-143.

López-Vizcaíno, R., Risco, C., Isidro, J., Rodrigo, S., Saez, C., Cañizares, P., Navarro, V., Rodrigo, M.A., 2017a. Scale-up of the electrokinetic fence technology for the removal of

pesticides. Part I: Some notes about the transport of inorganic species. Chemosphere 166, 540-548.

López-Vizcaíno, R., Risco, C., Isidro, J., Rodrigo, S., Saez, C., Cañizares, P., Navarro, V., Rodrigo, M.A., 2017b. Scale-up of the electrokinetic fence technology for the removal of pesticides. Part II: Does size matter for removal of herbicides? Chemosphere 166, 549-555.

López-Vizcaíno, R., Yustres, A., León, M.J., Saez, C., Cañizares, P., Rodrigo, M.A., Navarro, V., 2017c. Multiphysics Implementation of Electrokinetic Remediation Models for Natural Soils and Porewaters. Electrochim. Acta. 225, 93-104.

López-Vizcaíno, R., Yustres, A., Sáez, C., Cañizares, P., Rodrigo, M.A., Navarro, V., 2017d. Effect of polarity reversal on the enhanced electrokinetic remediation of 2,4-D-polluted soils: A numerical study. Electrochim. Acta. 258, 414-422

Mascia, M., Palmas, S., Polcaro, A.M., Vacca, A., Muntoni, A., 2007. Experimental study and mathematical model on remediation of Cd spiked kaolinite by electrokinetics. Electrochim. Acta. 52, 3360-3365.

Mitchell, J.K., Soga, K., 2005. Fundamentals of soil behavior. John Wiley & Sons, Inc, Hoboken, New Jersey, USA.

Ottosen, L.M., Hansen, H.K., Ribeiro, A.B., Villumsen, A., 2001. Removal of Cu, Pb and Zn in an applied electric field in calcareous and non-calcareous soils. J. Hazard. Mater. 85, 291-299.

Parkhurst, D.L., Appelo, C.A.J., 1999. User's guide to PHREEQ C (Version 2) – a computer program for speciation, batch-reaction, one-dimensional transport and inverse geochemical calculations, Water-Resources Investigations, Report 99–4259, Denver, Co. USA, 312.

Paz-García, J.M., Johannesson, B., Ottosen, L.M., Alshawabkeh, A.N., Ribeiro, A.B., Rodríguez-Maroto, J.M., 2012a. Modeling of electrokinetic desalination of bricks. Electrochim. Acta.86, 213-222.

Paz-García, J.M., Baek, K., Alshawabkeh, I.D., Alshawabkeh, A.N., 2012b. A generalized model for transport of contaminants in soil by electric fields. J. Environ. Sci. Health. Part A Toxic/Hazard. Subst. Environ. Eng. 47, 308-318.

Pazos, M., Rosales, E., Alcántara, T., Gómez, J., Sanromán, M.A., 2010. Decontamination of soils containing PAHs by electroremediation: A review. J. Hazard. Mater. 177, 1-11.

Pikal, M.J., 1971. Ion-pair formation and the theory of mutual diffusion in a binary electrolyte. J. Phys. Chem. 75, 663-675.

Puppala, S.K., Alshawabkeh, A.N., Acar, Y.B., Gale, R.J., Bricka, M., 1997. Enhanced electrokinetic remediation of high sorption capacity soil. J. Hazard. Mater. 55, 203-220.

Reddy, K.R., Cameselle, C., 2009. Electrochemical Remediation Technologies for Polluted Soils, Sediments and Groundwater. John Wiley and Sons.

Reddy, K.R., Parupudi, U.S., Devulapalli, S.N., Xu, C.Y., 1997. Effects of soil composition on the removal of chromium by electrokinetics. J. Hazard. Mater. 55, 135-158.

Rhoades, J.D., Manteghi, N.A., Shouse, P.J., Alves, W.J., 1989. Soil Electrical Conductivity and Soil Salinity: New Formulations and Calibrations. Soil Sci. Soc. Am. J. 53, 433-439.

Ribeiro, A.B., Mateus, E.P., Rodríguez-Maroto, J.M., 2011. Removal of organic contaminants from soils by an electrokinetic process: The case of molinate and bentazone. Experimental and modeling. Sep. Purif. Technol. 79, 193-203.

Ribeiro, A.B., Rodriguez-Maroto, J.M., Mateus, E.P., Gomes, H., 2005. Removal of organic contaminants from soils by an electrokinetic process: the case of atrazine. Experimental and modeling. Chemosphere 59, 1229-1239.

Risco, C., López-Vizcaíno, R., Sáez, C., Yustres, A., Cañizares, P., Navarro, V., Rodrigo, M.A., 2016a. Remediation of soils polluted with 2,4-D by electrokinetic soil flushing with facing rows of electrodes: A case study in a pilot plant. Chem. Eng. J. 285, 128-136.

Risco, C., Rodrigo, S., López-Vizcaíno, R., Sáez, C., Cañizares, P., Navarro, V., Rodrigo, M.A., 2016b. Electrokinetic flushing with surrounding electrode arrangements for the remediation of soils that are polluted with 2,4-D: A case study in a pilot plant. Sci. Total Environ. 545-546, 256-265.

Risco, C., Rodrigo, S., López-Vizcaíno, R., Yustres, A., Sáez, C., Cañizares, P., Navarro, V., Rodrigo, M.A., 2015. Electrochemically assisted fences for the electroremediation of soils polluted with 2,4-D: A case study in a pilot plant. Sep. Purif. Technol. 156, Part 2, 234-241.

Rodrigo, M.A., Oturan, N., Oturan, M.A., 2014. Electrochemically assisted remediation of pesticides in soils and water: a review. Chem. Rev. 114, 8720-8745.

Ryu, B.-G., Park, G.-Y., Yang, J.-W., Baek, K., 2011. Electrolyte conditioning for electrokinetic remediation of As, Cu, and Pb-contaminated soil. Sep. Purif. Technol. 79, 170-176.

Saichek, R.E., Reddy, K.R., 2003. Effect of pH control at the anode for the electrokinetic removal of phenanthrene from kaolin soil. Chemosphere 51, 273-287.

Steefel, C.I., Appelo, C.A.J., Arora, B., Jacques, D., Kalbacher, T., Kolditz, O., Lagneau, V., Lichtner, P.C., Mayer, K.U., Meeussen, J.C.L., Molins, S., Moulton, D., Shao, H., Šimůnek, J., Spycher, N., Yabusaki, S.B., Yeh, G.T., 2015. Reactive transport codes for subsurface environmental simulation. Comput. Geosci. 19, 445-478.

van Genuchten, M.T., 1980. A Closed-form Equation for Predicting the Hydraulic Conductivity of Unsaturated Soils1. Soil Sci. Soc. Am. J. 44, 892-898.

Vieira dos Santos, E., Sáez, C., Cañizares, P., Martínez-Huitle, C.A., Rodrigo, M.A., 2017. Reversible electrokinetic adsorption barriers for the removal of atrazine and oxyfluorfen from spiked soils. J. Hazard. Mater. 322, 413-420.

Vieira dos Santos, E., Souza, F., Saez, C., Cañizares, P., Lanza, M.R.V., Martinez-Huitle, C.A., Rodrigo, M.A., 2016. Application of electrokinetic soil flushing to four herbicides: A comparison. Chemosphere 153, 205-211.

Villen-Guzman, M., Paz-Garcia, J.M., Rodriguez-Maroto, J.M., Gomez-Lahoz, C., Garcia-Herruzo, F., 2014. Acid Enhanced Electrokinetic Remediation of a Contaminated Soil using Constant Current Density: Strong vs. Weak Acid. Sep. Sci. Technol. 49, 1461-1468.

Virkutyte, J., Sillanpaa, M., Latostenmaa, P., 2002. Electrokinetic soil remediation - critical overview. Sci. Total Environ. 289, 97-121.

Yeung, A.T., Gu, Y.Y., 2011. A review on techniques to enhance electrochemical remediation of contaminated soils. J. Hazard. Mater. 195, 11-29.

Yustres, Á., López-Vizcaíno, R., Sáez, C., Cañizares, P., Rodrigo, M.A., Navarro, V., 2018. Water transport in electrokinetic remediation of unsaturated kaolinite. Experimental and numerical study. Sep. Purif. Technol. 192, 196-204.

Zhou, D.M., Alshawabkeh, A.N., Deng, C.F., Cang, L., Si, Y.B., 2004a. Electrokinetic removal of chromium and copper from contaminated soils by lactic acid enhancement in the catholyte. J. Environ. Sci. 16, 529-532.

Zhou, D.M., Deng, C.F., Cang, L., 2004b. Electrokinetic remediation of a Cu contaminated red soil by conditioning catholyte pH with different enhancing chemical reagents. Chemosphere 56, 265-273.

SUPPLEMENTARY MATERIAL

Enhanced Electrokinetic Remediation of Polluted Soils by Anolyte pH Conditioning

López Vizcaíno, R.[a*], Yustres, A.[a], Asensio, L.[a], Saez, C.[b], Cañizares, P.[b], Rodrigo, M.A.[b], Navarro, V.[a]

[a]University of Castilla-La Mancha - Institute of Technology, Campus Universitario s/n, 16071 Cuenca, Spain

[b]Department of Chemical Engineering, Faculty of Chemical Sciences & Technologies, University of Castilla-La Mancha, Campus Universitario s/n, 13071 Ciudad Real, Spain

*** Corresponding author:** ruben.lopezvizcaino@uclm.es; r.lopezvizcaino@gmail.com, University of Castilla-La Mancha - Institute of Technology, Campus Universitario s/n, 16071 Cuenca, Spain

Table SM-1. Soil parameters**.**

Parameter categories	Parameters	Description	Values	Units
Water retention curve parameters	α_{VG}	Parameter of the van Genuchten retention curve	0.0147	kPa^{-1}
	n_{VG}	Parameter of the van Genuchten retention curve	1.2593	-
	m_{VG}	Parameter of the van Genuchten retention curve	0.2059	-
Soil structural parameters	ϕ	Porosity	0.4681	-
	ρ_s	Soil particle density	2681.5	$kg\ m^{-3}$
	$\mathcal{D}_i^L$	Longitudinal dispersivity of species *i*	0.01	m
	τ	Tortuosity	1.00	-
Water flow parameters	K_{sat}^{h}	Saturated hydraulic permeability	2.03×10^{-10}	$m\ s^{-1}$
	K_{sat}^{eo}	Saturated electroosmotic permeability	2.4×10^{-9}	$m^2\ V^{-1}\ s^{-1}$

Table SM-2. Thermodynamic properties of the modelled geochemical systems.

Species categories	Species	Reactions	logK^{eq} (25ºC)	Hard-core diameter / Å	D^o / m^2s^{-1}
Components	Cl^-	Cl^-	0	3.6	2.03×10^{-9}
	H_2O	H_2O	0	3.4	5.27×10^{-9}
	H^+	H^+	0	4.1	9.31×10^{-9}
	Na^+	Na^+	0	4.1	1.33×10^{-9}
	2,4-D^-	2,4-D^-	0	3.4	6.50×10^{-10}
Secondary species	OH^-	$H_2O \leftrightarrow OH^- + H^+$	-14	3.6	5.27×10^{-9}
	NaOH	$Na^+ + H_2O \leftrightarrow NaOH + H^+$	-14.75	3.4	$1.89\times10^{-10*}$
	NaCl	$Na^+ + Cl^- \leftrightarrow NaCl$	-0.5	3.4	$1.89\times10^{-10*}$
	2,4-D	2,4-D^- + $H^+ \leftrightarrow$ 2,4-D	2.73	3.4	6.50×10^{-10}

* Obtained using Pikal's model (Pikal, 1971)

Table SM-3. Test planning.

Test	Code	[NaOH] in FF / m	Test time / h
Reference test	T-0	0	89
A-pH-C test 1	T-1	0.01	262
A-pH-C test 2	T-2	0.0125	460
A-pH-C test 3	T-3	0.015	421
A-pH-C test 4	T-4	0.0175	261
A-pH-C test 5	T-5	0.02	166
A-pH-C test 6	T-6	0.025	104